Towards Einstein-Podolsky-Rosen quantum channel multiplexing

Boris Hage, Aiko Samblowski, and Roman Schnabel*

Institut für Gravitationsphysik, Leibniz Universität Hannover, and Max-Planck-Institut für Gravitationsphysik (Albert-Einstein-Institut), Callinstr. 38, D-30167 Hannover, Germany

(Received 13 December 2009; published 1 June 2010)

A single broadband squeezed field constitutes a quantum communication resource that is sufficient for the realization of a large number N of quantum channels based on distributed Einstein-Podolsky-Rosen entangled states. Each channel can serve as a resource for, for example, independent quantum key distribution or teleportation protocols. N-fold channel multiplexing can be realized by accessing $2N$ squeezed modes at different Fourier frequencies. We report on the experimental implementation of the $N = 1$ case through the interference of two squeezed states, extracted from a single broadband squeezed field, and demonstrate all techniques required for multiplexing ($N > 1$). Quantum channel frequency multiplexing can be used to optimize the exploitation of a broadband squeezed field in a quantum information task. For instance, it is useful if the bandwidth of the squeezed field is larger than the bandwidth of the homodyne detectors. This is currently a typical situation in many experiments with squeezed and two-mode squeezed entangled light.

DOI: 10.1103/PhysRevA.81.062301 PACS number(s): 03.67.Hk, 03.65.Ud, 03.67.Mn, 42.50.Dv

I. INTRODUCTION

Einstein-Podolsky-Rosen (EPR) entangled [1] optical states can be used to constitute quantum communication channels between two distant parties. Such channels have been successfully demonstrated in both complementary regimes of light. Entanglement in the degrees of freedom of photons can be produced by parametric down-conversion and conditional single-photon detection [2,3]. This is the discrete variable regime, in which, more generally, arbitrary photon number states with conditional or unconditional detection might be involved. Entanglement in the degrees of freedom of waves, that is, the field quadratures, provide quantum correlations in variables possessing a continuous measurement spectrum [4–8]. In both regimes, applications of entangled states in quantum teleportation [9–12] and quantum key distribution [13–16] have attracted much attention. Continuous variable (CV) quantum communication is in direct analogy to conventional communication schemes in which information is encoded in amplitude modulations and phase (frequency) modulations of a, possibly continuous, carrier wave. The amount of quantum information that can be transmitted, for example, to generate a secret key for quantum cryptography, is proportional to the bandwidth used. However, the usable entanglement bandwidth of a channel is typically not limited by the CV entangled field itself but, rather, by the speed of the high-quantum-efficiency homodyne detectors. Recently, Mehmet *et al.* [17] demonstrated a broadband squeezed field with a nonclassical noise supression of up to 11.5 dB and a bandwidth as large as 170 MHz. However, for Fourier frequencies above a couple of tens of megahertz, strong squeezing could only be observed after the dark noise of the balanced homodyne detector was subtracted. EPR quantum channel frequency multiplexing is a tool to overcome the detection bandwidth limitation.

Schori *et al.* [18] demonstrated experimentally that EPR entanglement can be produced from two frequency modes of a squeezed field. In their experiment two *narrowband* longitudinal cavity modes of an optical parametric oscillator were separated with filter cavities and their correlations were detected with two balanced homodyne detectors that used frequency-shifted local oscillators. Later Zhang [19] proposed splitting a single *broadband* squeezed cavity mode into N pairs of upper and lower single sideband fields and to demonstrate N independent EPR entangled modulation fields.

In this paper we report on the experimental generation of an EPR quantum channel from a broadband squeezed field, which corresponds to the $N = 1$ case as proposed in Ref. [19]. In our experiment the complete set of building blocks required for future CV EPR quantum channel multiplexing ($N > 1$) is demonstrated. A multiplication of solely the classical resources of our experiment will allow the establishment of a linearly increasing number of EPR quantum channels between pairs of distant parties from a single broadband squeezed field.

II. DEMONSTRATION OF THE EINSTEIN-PODOLSKY-ROSEN PARADOX

In previous continuous-wave experiments CV EPR entanglement has been efficiently produced either by type II optical parametric amplification (OPA) [5,21–23] or by the interference of two squeezed outputs from two type I OPA processes on a 50:50 beam splitter [7,8,11,12,24]. Quite generally, bipartite CV, Gaussian entangled states can be represented by the two spatial output modes of a 50:50 beam splitter, as the result of the interference of two squeezed input modes. The states under consideration are sideband modulation fields at frequency Ω_{EPR} with bandwidth $\Delta\Omega$, carried by an optical field of frequency ω_0, and are formally described in the rotating frame by noncommuting pairs of time-dependent quadrature operators $\hat{X}(\Omega_{\mathrm{EPR}},\Delta\Omega,t)$ and $\hat{X}^{\perp}(\Omega_{\mathrm{EPR}},\Delta\Omega,t)$, respectively, with $\Delta\Omega/2 < \Omega_{\mathrm{EPR}} \ll \omega_0$. In most CV EPR entanglement experiments so far, two optical frequencies ($\omega_0 \pm \Omega_{\mathrm{EPR}}$) have been involved.

In this work we used a single broadband squeezed field to realize EPR entanglement. In this case, in a total of four

*roman.schnabel@aei.mpg.de

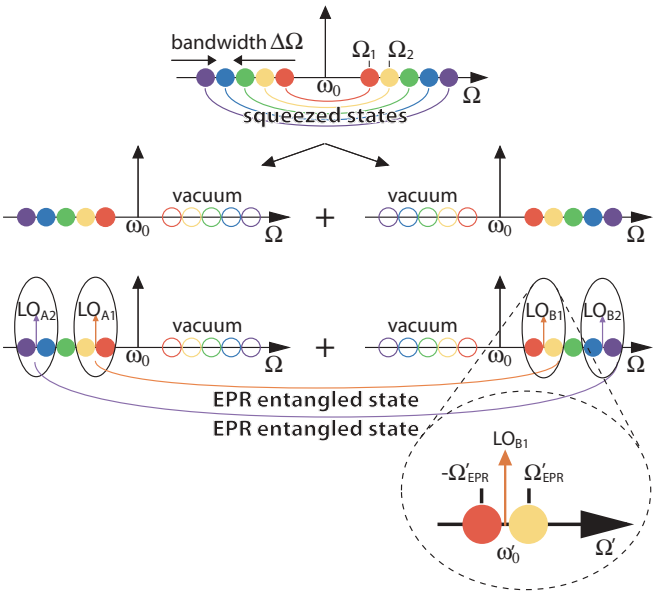

FIG. 1. (Color online) Scheme for the generation of EPR entanglement from a single broadband squeezed field in the rotating frame ($\omega_0 = 0$). Top: Squeezed states in Fourier frequency space described as the sum of quantum correlated upper and lower sideband pairs with resolution bandwidths corresponding to the circles' diameters. Center line: Splitting of the squeezed states by a frequency beam splitter, that is, filter cavity. Bottom: Adding pairs of frequency-shifted local oscillators provides EPR entanglement due to interference of the squeezed states at two different Fourier frequencies. Inset: Fourier frequencies defined in the system $\omega_0' = 0$.

different optical frequencies contributed to the generation of an EPR entangled state, as shown for the two entangled states in the lower pictures in Fig. 1. For this reason, such an EPR state was named a *four-mode squeezed state* in [20]. However, as in other bipartite quadrature entangled states, the entanglement is observed between two spatial modes at a single modulation frequency, Ω'_{EPR}. The distinct feature is that here, Ω'_{EPR} is defined with respect to two local oscillators with different optical frequencies. The top picture in Fig. 1 shows that modulation fields being in squeezed states can be described as the beats between pairs of quantum correlated upper and lower optical sideband fields at frequencies $\omega_0 \pm \Omega_i$ [25]. For this reason, a squeezed state (of a modulation field) has sometimes been called a *two-mode squeezed state* [26]. We note that a Gaussian (bipartite) EPR entangled state has also been called a two-mode squeezed state to pinpoint the presence of quantum correlations in the two spatial modes.

In our experiment a single broadband squeezed field at 1064 nm was generated in a half-monolithic (hemilithic), single-ended standing-wave nonlinear cavity using type I OPA [27]. The nonlinear medium inside the cavity was a 7% magnesium oxide-doped lithium niobate (7% MgO:$LiNbO_3$) crystal that was pumped with 65 mW of continuous-wave laser radiation at 532 nm. The effective length of the cavity was 39 mm and the coupler reflectivity was $r^2 = 95.7\%$. The squeezing strength observed was approximately 5.5 dB for Fourier frequencies from 4 to 10 MHz. At higher frequencies the squeezing strength degraded due to the finite bandwidth of the OPA cavity, which was 25 MHz. At lower frequencies

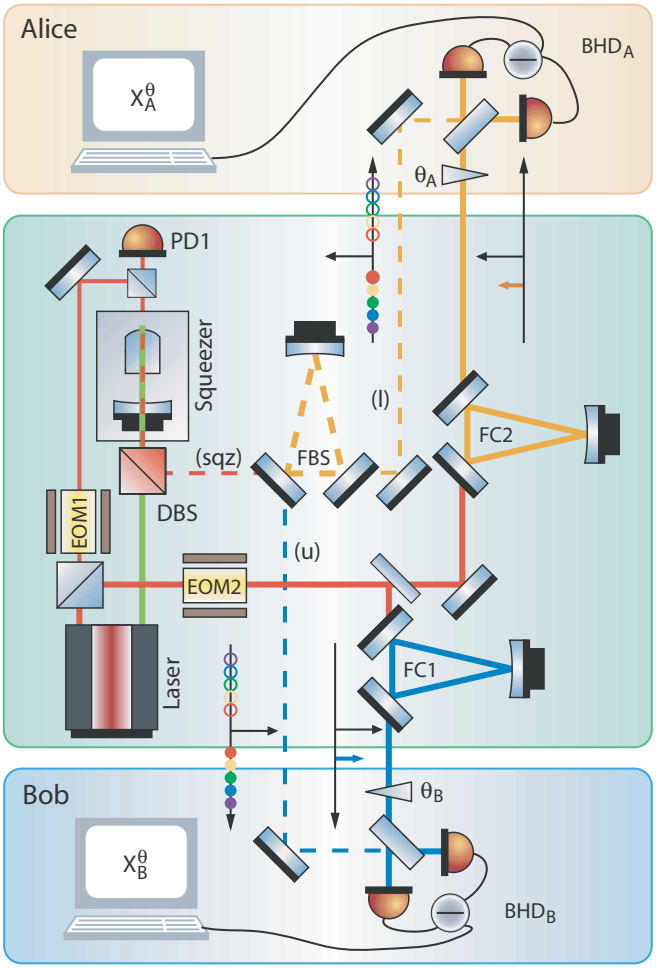

FIG. 2. (Color online) Experimental setup to establish an EPR quantum channel ($N = 1$) from a single squeezed beam (sqz). The triangular filter cavity FBS was used as a frequency beam splitter to separate the upper [(u); blue] from the lower [(l); orange] sidebands of the nonclassical field. The electro-optical modulator EOM1 and photodiode PD1 were used for controlling the OPA cavity length and the pump-field phase. DBS was a dichroic beam splitter, which reflected 1064 nm and transmitted 532 nm radiation. EOM2 generated bright sidebands by a deep phase modulation at 7 MHz. These sidebands served as LOs in Alice's and Bob's homodyne detectors (BHDs). FC1 was tuned to transmit the upper sideband at +7 MHz; FC2 transmits the lower one at −7 MHz.

classical noise from control beams that sensed the OPA cavity length and the orientation of the squeezing ellipse degraded the squeezing strength. This noise may be significantly reduced by appropriate control schemes [28].

The generation of EPR entanglement from a single broadband squeezed field requires the implementation of the interference of two squeezed states defined at different Fourier frequencies. To achieve this, altogether three triangular traveling wave filter cavities were employed (FBS, FC1, and FC2); see Fig. 2. All three filter cavities consisted of three dielectrically coated low-loss mirrors. The two plane input-output coupling mirrors had a power transmission of $T = 8500$ ppm for p- and $T = 300$ ppm for s-polarized light. The curved cavity end mirror showed a transmission of $T = 5$ ppm. This provided finesse values of $\mathcal{F}_p = 370$ for p

and $\mathcal{F}_s = 10\,500$ for s polarization and linewidths of 1.5 MHz and 55 kHz, respectively, in accordance with the round-trip length of 52 cm. The resonators were almost lossless and transmitted more than 95% resonant light power. The lengths of the cavities were controlled via piezo electric transducers. The filter cavity FBS was used as a frequency beam splitter that spatially separated the upper and lower sideband components of the broadband squeezed field (Fig. 2). The filter cavity FBS was operated in its low-finesse mode and was detuned by -7 MHz with respect to the carrier field at 1064 nm. Hence it transmitted the fields around -7 MHz (lower sidebands) and reflected the rest, particularly the upper sidebands around $+7$ MHz. The upper sidebands were sent to Bob's balanced homodyne detector (BHD) with a local oscillator (LO), which was frequency shifted by $+7$ MHz but, nevertheless, had a constant phase with respect to the main carrier field. The lower sidebands at Alice's site were detected with a LO at -7 MHz. We note that the splitting of upper and lower sidebands of a broadband squeezed field has been demonstrated before [29]. The LOs for Alice's and Bob's BHDs were generated by electro-optic phase modulation of a part of the carrier field (EOM2 in Fig. 2) and subsequent filtering (FC1 and FC2). The modulation frequency was 7 MHz. About one third of the power of the carrier was transferred into sidebands at ± 7 MHz. The modulated beam was then split into two by a 50:50 power beam splitter. Each of these was sent to an optical filter cavity, FC1 and FC2, respectively. Both cavities were operated in high-finesse mode. Again, these resonators were detuned to $+7$ and -7 MHz, respectively, and hence transmitted only the corresponding sideband. The power of the carrier was suppressed by a factor of 10^5, which was sufficiently high to measure quadrature operators in the frequency-shifted reference frames at Alice's and Bob's site. Both BHDs could be phase locked to arbitrary quadrature angles. The error signals for these control loops were derived from the beat between the LOs and the week carrier fields copropagating with the correlated sideband fields. In particular, the control loops allowed the subsequent measurement of orthogonal quadrature phases. Both BHD signals were demodulated at 200 kHz, low pass filtered at 50 kHz, and fed into a data acquisition system. Calculation of the variances of each signal, the variance of the sum or difference, and the covariances of the two signals was conducted with PC software. Electronic noise of the measurement and data acquisition devices were at least a factor of 10 smaller than quadrature signals and did not need to be taken into account.

To witness the presence of entanglement in our experiment, we followed [7] and [30] and applied the inseparability criterion introduced by Duan *et al.* [31] and the EPR criterion introduced by Reid and Drummond [32]. For our setup the inseparability criterion for the presence of entanglement in the quadratures of two fields can be written in the following form [7,31]:

$$\mathcal{I}_{\text{Insep}} = \tfrac{1}{4}[V(\hat{X}_A - \hat{X}_B) + V(\hat{X}_A^{\perp} + \hat{X}_B^{\perp})] < 1. \qquad (1)$$

Here V denotes variances, with the variance of a vacuum field normalized to unity. $\hat{X}_A$ and $\hat{X}_B$ are the fields' quadrature phase operators at Alice's and Bob's site for which the variance of their difference $V(\hat{X}_A - \hat{X}_B)$ is minimal. $\hat{X}_A^{\perp}$ and $\hat{X}_B^{\perp}$ are the quadrature phase operators orthogonal to $\hat{X}_A$ and $\hat{X}_B$, respectively.

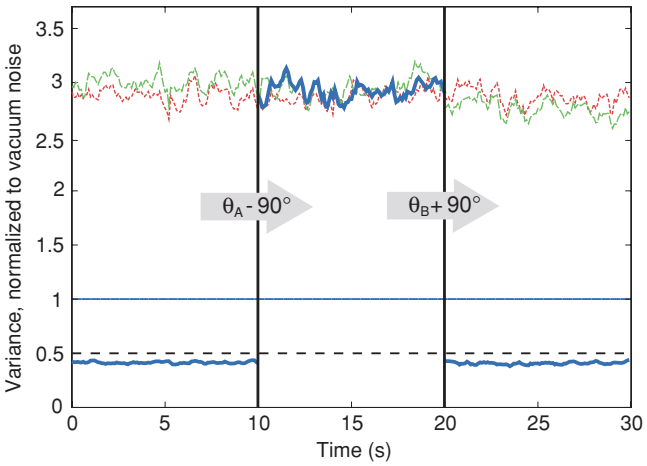

FIG. 3. (Color online) Demonstration of strong entanglement between two laser fields at Alice's and Bob's sites. The two lower measurement traces correspond to half the variances in Eq. (1), thereby fulfilling the inequality with $\mathcal{I}_{\text{Insep}} \approx 0.4 < 1$. The dashed traces correspond to the variances measured on the individual beams.

Figure 3 presents consecutive measurement time series of $V(\hat{X}_A)$, $V(\hat{X}_B)$, and $(1/2)V(\hat{X}_A - \hat{X}_B)$ (left), $V(\hat{X}_A)$, $V(-\hat{X}_B^{\perp})$ and $(1/2)V(\hat{X}_A + \hat{X}_B^{\perp})$ (center), and $V(\hat{X}_A^{\perp})$, $V(-\hat{X}_B^{\perp})$, and $(1/2)V(\hat{X}_A^{\perp} + \hat{X}_B^{\perp})$ (right). During the measurement time shown, the BHDs at Alice's and Bob's site were phase controlled and were quickly and sequentially switched from an $\hat{X}$ to an $\hat{X}^{\perp}$ measurement. Additionally, the vacuum noise levels of the detectors were measured and used to normalize the traces shown. Using Eq. (1), the data in Fig. 3 clearly demonstrate the presence of entanglement with $\mathcal{I}_{\text{Insep}} = 0.41 \pm 0.02$. This value not only fulfills the inequality, but also is lower than 0.5, proving that less than a full unit of vacuum noise entered the detection of entanglement in our setup. In this case the entanglement is strong enough to observe the EPR paradox. By optimizing the gain factors in subsequent measurement results for two noncommuting quadratures on Bob's field, we were able to infer the corresponding results on Alice's field more precisely than suggested by the existence of vacuum noise. The EPR paradox is observed if the following EPR criterion is fulfilled [32]:

$$\mathcal{E}_{\text{EPR}} = \min_{g} \langle (\delta\hat{X}_A - g\,\delta\hat{X}_B)^2 \rangle \times \min_{g^{\perp}} \langle (\delta\hat{X}_A^{\perp} + g^{\perp}\delta\hat{X}_B^{\perp})^2 \rangle < 1\,, \qquad (2)$$

with $\delta\hat{X} = \hat{X} - \langle\hat{X}\rangle$ and g and $g^{\perp}$ being parameters that are experimentally adjusted to minimize the two expectation values in Eq. (2). We observed a value of $\mathcal{E}_{\text{EPR}} = 0.64 \pm 0.02$.

III. DISCUSSION

In our experiment two squeezed states at Fourier frequencies of $\Omega_1 = 6.8$ MHz and $\Omega_2 = 7.2$ MHz with bandwidths of $\Delta\Omega = 2 \times 50$ kHz were brought to interference to produce

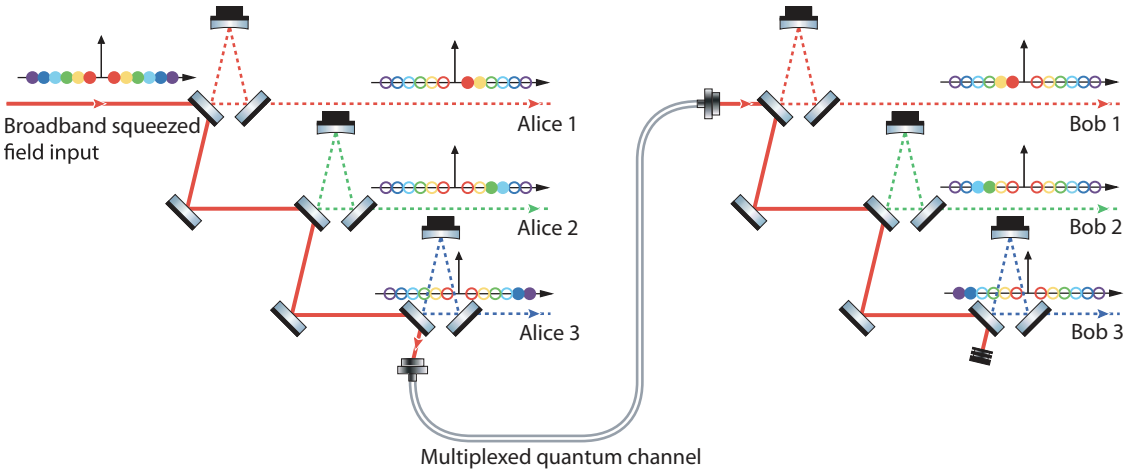

FIG. 4. (Color online) Lower sidebands of a broadband squeezed field are sent to a remote receiver (Bob), thereby establishing a quantum channel for the distribution of entanglement. The distributed entanglement can be used to generate a quantum key that is shared between the sender and the receiver. Multiplexing divides the channel's capacity into several (here, into $N = 3$) channels. Each channel uses a distinct frequency range, distributes EPR entanglement, and can be used to generate a quantum key. In this way several data streams are combined into one transmission medium. The establishment of another frequency range requires an additional pair of filter cavities and an additional pair of frequency-shifted local oscillators (not shown).

an EPR entangled state at the Fourier frequency of $\Omega'_{\mathrm{EPR}} = 200$ kHz with respect to the frequency-shifted LOs. The initial squeezed states were carried by a single broadband squeezed field. The same field carried more squeezed states that were not used by our quantum channel. Figure 4 shows how a single broadband squeezed field can be used to provide the nonclassical resource of three ($N = 3$ multiplexed) EPR quantum channels. Each channel can be used for quantum communication tasks between Alice and Bob or, alternatively, can be established between different senders and receivers. Quantum channel frequency multiplexing can be used if the individual quantum communication tasks require less bandwidth than provided by the entangled light source. However, a more obvious application is to overcome the bandwidth limitations set by balanced homodyne detectors. In principle, the bandwidth of a squeezed light source design is limited just by the available second harmonic pump power and by the phase-matching bandwidth of the nonlinear material used. For periodically poled materials such as PPKTP, the phase-matching bandwidth is of the order of a nanometer and can therefore cover hundreds of gigahertz [33]. High-quantum-efficiency BHDs with low electronic noise used in nonclassical light applications typically have detection bandwidths of just several tens of megahertz, because faster BHDs require smaller photodiodes and, consequently, optical LOs with less power, to avoid excessively high thermal loads (see, e.g., [34]). A significant increase in bandwidth is certainly possible, however, the optical bandwidths of nonclassical light sources will probably not be reached. Multiplexing of the nonclassical frequency band can solve this gap. N pairs of frequency-shifted LOs picked from a frequency comb with a frequency separation of twice the electronic detection bandwidth can complement the scheme shown in Fig. 4. Thus high-speed quantum communication with N times the electronic detection bandwidth can be achieved.

IV. SUMMARY

To summarize, we experimentally demonstrated that a single broadband squeezed field can be used to establish an EPR quantum channel. Additional EPR quantum channels can be produced by increasing the classical resources of our experiment without increasing its nonclassical resources. The EPR quantum channel multiplexing discussed will allow efficient use of broadband nonclassical fields for the realization of ultrahigh quantum information transmission rates.

ACKNOWLEDGMENTS

We thank U. Andersen, R. Fillip, J. Fiurášek, N. Lastzka, and G. Leuchs for many helpful discussions regarding entanglement of sideband fields and J. DiGuglielmo, A. Franzen, and H. Vahlbruch for discussions regarding the control of entangled quadrature phases. We would like to acknowledge financial support from the Deutsche Forschungsgemeinschaft through the SFB407.

[1] A. Einstein, B. Podolsky, and N. Rosen, Phys. Rev. **47**, 777 (1935).
[2] Z. Y. Ou and L. Mandel, Phys. Rev. Lett. **61**, 50 (1988).
[3] P. G. Kwiat, K. Mattle, H. Weinfurter, A. Zeilinger, A. V. Sergienko, and Y. Shih, Phys. Rev. Lett. **75**, 4337 (1995).
[4] M. D. Reid, Phys. Rev. A **40**, 913 (1989).
[5] Z. Y. Ou, S. F. Pereira, H. J. Kimble, and K. C. Peng, Phys. Rev. Lett. **68**, 3663 (1992)
[6] C. Silberhorn, P. K. Lam, O. Weiß, F. König, N. Korolkova, and G. Leuchs, Phys. Rev. Lett. **86**, 4267 (2001).

[7] W. P. Bowen, R. Schnabel, P. K. Lam, and T. C. Ralph, Phys. Rev. Lett. **90**, 043601 (2003).
[8] J. DiGuglielmo, B. Hage, A. Franzen, J. Fiurášek, and R. Schnabel, Phys. Rev. A **76**, 012323 (2007).
[9] D. Bouwmeester *et al.*, Nature **390**, 575 (1997).
[10] D. Boschi, S. Branca, F. DeMartini, L. Hardy, and S. Popescu, Phys. Rev. Lett. **80**, 1121 (1998).
[11] A. Furusawa, J. L. Sørensen, S. L. Braunstein, C. A. Fuchs, H. J. Kimble, and E. S. Polzik, Science **282**, 706 (1998).
[12] W. P. Bowen, N. Treps, B. C. Buchler, R. Schnabel, T. C. Ralph, H.-A. Bachor, T. Symul, and P. K. Lam, Phys. Rev. A **67**, 032302 (2003).
[13] C. H. Bennett *et al.*, J. Cryptol. **5**, 3 (1992).
[14] T. Jennewein, C. Simon, G. Weihs, H. Weinfurter, and A. Zeilinger, Phys. Rev. Lett. **84**, 4729 (2000).
[15] K. Bencheikh *et al.*, J. Mod. Opt. **48**, 1903 (2001).
[16] R. García-Patrón and N. J. Cerf, Phys. Rev. Lett. **97**, 190503 (2006).
[17] M. Mehmet, H. Vahlbruch, N. Lastzka, K. Danzmann, and R. Schnabel, Phys. Rev. A **81**, 013814 (2010).
[18] C. Schori, J. L. Sørensen, and E. S. Polzik, Phys. Rev. A **66**, 033802 (2002).
[19] Jing Zhang, Phys. Rev. A **67**, 054302 (2003).
[20] B. L. Schumaker, S. H. Perlmutter, R. M. Shelby, and M. D. Levenson, Phys. Rev. Lett. **58**, 357 (1987).
[21] J. Laurat, T. Coudreau, G. Keller, N. Treps, and C. Fabre, Phys. Rev. A **71**, 022313 (2005).
[22] X. Su, A. Tan, X. Jia, J. Zhang, C. Xie, and K. Peng, Phys. Rev. Lett. **98**, 070502 (2007).
[23] A. S. Villar, L. S. Cruz, K. N. Cassemiro, M. Martinelli, and P. Nussenzveig, Phys. Rev. Lett. **95**, 243603 (2005).
[24] H. Yonezawa, S. L. Braunstein, and A. Furusawa, Phys. Rev. Lett. **99**, 110503 (2007).
[25] H.-A. Bachor and T. C. Ralph, *A Guide to Experiments in Quantum Optics*, 2nd ed. (Wiley-VCH, Weinheim, 2004).
[26] B. L. Schumaker and C. M. Caves, Phys. Rev. A **31**, 3093 (1985).
[27] S. Chelkowski, H. Vahlbruch, K. Danzmann, and R. Schnabel, Phys. Rev. A **75**, 043814 (2007).
[28] H. Vahlbruch, S. Chelkowski, B. Hage, A. Franzen, K. Danzmann, and R. Schnabel, Phys. Rev. Lett. **97**, 011101 (2006).
[29] E. H. Huntington, G. N. Milford, C. Robilliard, T. C. Ralph, O. Glöckl, U. L. Andersen, S. Lorenz, and G. Leuchs, Phys. Rev. A **71**, 041802(R) (2005).
[30] W. P. Bowen, R. Schnabel, P. K. Lam, and T. C. Ralph, Phys. Rev. A **69**, 012304 (2004).
[31] L-M. Duan, G. Giedke, J. I. Cirac, and P. Zoller, Phys. Rev. Lett. **84**, 2722 (2000).
[32] M. D. Reid and P. D. Drummond, Phys. Rev. Lett. **60**, 2731 (1988).
[33] R. W. Boyd, *Nonlinear Optics*, 2nd ed. (CRC Press, Boca Raton, FL, 2003); V. Pasiskevicius, I. Freitag, H. Karlsson, J. Hellström, and F. Laurell, Proc. SPIE **3928**, 2 (2000).
[34] P. C. D. Hobbs, *Building Electro-Optical Systems, Making it all Work* (John Wiley & Sons, New York, 2000).